Technische Universität Berlin
Institut für Mathematik

M007 - A Skateboard(v1.0)

Andreas Steinbrecher

Preprint 2016/08

Preprint-Reihe des Instituts für Mathematik
Technische Universität Berlin
http://www.math.tu-berlin.de/preprints

Report 2016/08 **February 2016**

The considerations in this report *A Skateboard* are part of the example collection which can be found in `http://www3.math.tu-berlin.de/multiphysics/Examples/`. The aim is to investigate different formulations, i.e., regularized formulations or also index reduced formulations, of the model equations in combination with different numerical solvers with respect to its applicability, efficiency, accuracy, and robustness.

AMS(MOS) subject classification: 65L80

Keywords: example collection, numerical integration, differential-algebraic equations

Authors address:

Andreas Steinbrecher
Institut für Mathematik
Sekretariat MA 4-5
Technische Universität Berlin
10623 Berlin
Germany
`anst@math.tu-berlin.de`

M007 - A Skateboard[‡](v1.0)

Andreas Steinbrecher[§]

February 18, 2016

Abstract

The considerations in this report *A Skateboard* are part of the example collection which can be found in `http://www3.math.tu-berlin.de/multiphysics/Examples/`. The aim is to investigate different formulations, i.e., regularized formulations or also index reduced formulations, of the model equations in combination with different numerical solvers with respect to its applicability, efficiency, accuracy, and robustness.

Keywords: example collection, numerical integration, differential-algebraic equations

AMS(MOS) subject classification: 65L80

1 Introduction

The considerations in this report *A Skateboard* are part of the example collection which can be found in `http://www3.math.tu-berlin.de/multiphysics/Examples/`. The aim is to investigate different formulations, i.e., regularized formulations or also index reduced formulations, of the model equations in combination with different numerical solvers with respect to its applicability, efficiency, accuracy, and robustness.

2 A Skateboard

In this example we will consider a skateboarder who is driving on a flat horizontal surface. The simplified topology is illustrated in Figure 1.

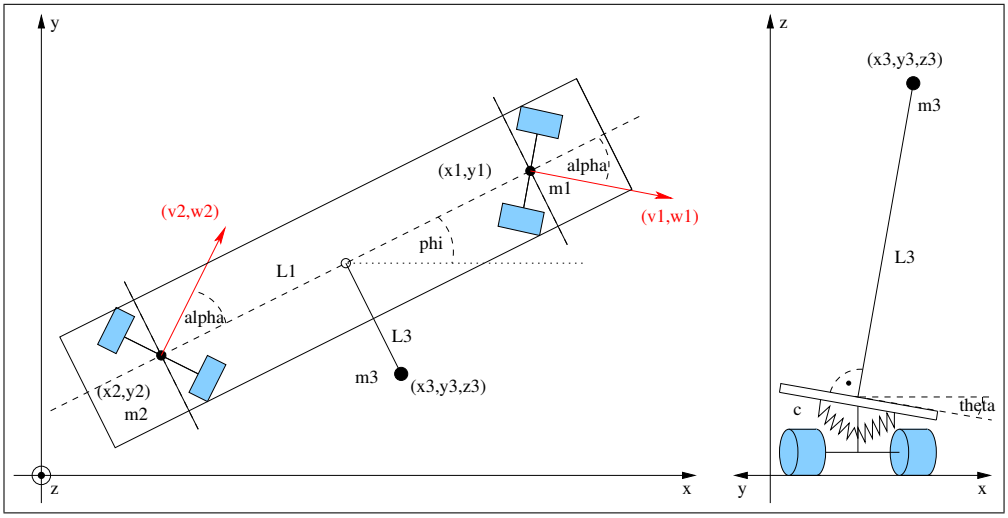

Figure 1: Topology

[‡]This work has been supported by European Research Council through Advanced Grant "Modeling, Simulation and Control of Multi-Physics Systems" (MODSIMCONMP)

[§]Institut für Mathematik, Sekretariat MA 4-5, Technische Universität Berlin, 10623 Berlin, Germany, `anst@math.tu-berlin.de`

2.1 Model equations

2.1.1 The Mathematical Model

The mathematical model corresponds to a semi-implicit DAE of strangeness index (s-index) $\nu_s = 2$, of differentiation index (d-index) $\nu_d = 3$, and of maximal constraint level (c-level) $\nu_c = 2$ consisting of 25 unknowns, 25 equations, comprising 18 differential equations and 7 algebraic equations. The model equations for the skateboard have the form

$$\begin{aligned} \dot{p} &= v, && \text{(1a)} \\ M\dot{v} &= f(p,v) - G^T(p)\lambda - H^T(p)\mu, && \text{(1b)} \\ 0 &= g(p), && \text{(1c)} \\ 0 &= H(p)v && \text{(1d)} \end{aligned}$$

with $p = \begin{bmatrix} x_1 & y_1 & x_2 & y_2 & \varphi & x_3 & y_3 & z_3 & \theta \end{bmatrix}^T$ and $v = \begin{bmatrix} v_1 & w_1 & v_2 & w_2 & \omega & v_3 & w_3 & u_3 & \psi \end{bmatrix}^T$ for $t \in \mathbb{I}$ with the time domain $\mathbb{I} = [t_0, t_f]$ and initial values $p(t_0) = p_0 \in \mathbb{R}^9$, $v(t_0) = v_0 \in \mathbb{R}^9$, $\lambda(t_0) = \lambda_0 \in \mathbb{R}^5$, and $\mu(t_0) = \mu_0 \in \mathbb{R}^2$. Furthermore, we have

$$M = \begin{bmatrix} m_1 & & & & & & & & \\ & m_1 & & & & & & & \\ & & m_2 & & & & & & \\ & & & m_2 & & & & & \\ & & & & J_1 & & & & \\ & & & & & m_3 & & & \\ & & & & & & m_3 & & \\ & & & & & & & m_3 & \\ & & & & & & & & J_2 \end{bmatrix}, \quad f(p,v) = \begin{bmatrix} -d_1 v_1 \\ -d_1 w_1 \\ -d_2 v_2 \\ -d_2 w_2 \\ -d_\varphi \omega \\ -d_3 v_3 \\ -d_3 w_3 \\ -m_3 \mathfrak{g} - d_3 u_3 \\ -c\theta - d_\theta \psi \end{bmatrix},$$

$$g(p) = \begin{bmatrix} x_2 + L_1 \cos(\varphi) - x_1 \\ y_2 + L_1 \sin(\varphi) - y_1 \\ (x_1 + x_2)/2 + L_3 \cos(\varphi - \pi/2)\sin(\theta) - x_3 \\ (y_1 + y_2)/2 + L_3 \sin(\varphi - \pi/2)\sin(\theta) - y_3 \\ L_3 \cos(\theta) - z_3 \end{bmatrix},$$

$$G(p) = \begin{bmatrix} -1 & 0 & 1 & 0 & -L_1 \sin(\varphi) & 0 & 0 & 0 & 0 \\ 0 & -1 & 0 & 1 & L_1 \cos(\varphi) & 0 & 0 & 0 & 0 \\ 1/2 & 0 & 1/2 & 0 & -L_3 \sin(\varphi - \pi/2)\sin(\theta) & -1 & 0 & 0 & L_3 \cos(\varphi - \pi/2)\cos(\theta) \\ 0 & 1/2 & 0 & 1/2 & L_3 \cos(\varphi - \pi/2)\sin(\theta) & 0 & -1 & 0 & L_3 \sin(\varphi - \pi/2)\cos(\theta) \\ 0 & 0 & 0 & 0 & 0 & 0 & 0 & -1 & -L_3 \sin(\theta) \end{bmatrix}, \text{ and}$$

$$H^T(p) = \begin{bmatrix} (x_1 - x_2)\cos(\pi/2 - \alpha) - (y_1 - y_2)\sin(\pi/2 - \alpha) & 0 \\ (x_1 - x_2)\sin(\pi/2 - \alpha) + (y_1 - y_2)\cos(\pi/2 - \alpha) & 0 \\ 0 & (x_1 - x_2)\cos(\pi/2 + \alpha) - (y_1 - y_2)\sin(\pi/2 + \alpha) \\ 0 & (x_1 - x_2)\sin(\pi/2 + \alpha) + (y_1 - y_2)\cos(\pi/2 + \alpha) \\ 0 & 0 \\ 0 & 0 \\ 0 & 0 \\ 0 & 0 \\ 0 & 0 \end{bmatrix},$$

where $\alpha = a\theta$. The unknown and auxiliary variables as well as the model parameters are listed in Tables 1, 2, and 3, respectively.

2.1.2 The Origin of the Problem

Let us model the board such that the whole mass of the board is split into the masses m_1 and m_2 located in the center of both axes whose positions are defined by (x_1, y_1) and (x_2, y_2), respectively. Furthermore, the orientation of the board is defined by the angle φ which gives the direction of the motion and by the angle θ which defines the bank of the board. It is assumed that the wheels of the skateboard do not

variable	physical meaning	unit	dimension
x_1	x-position of the front axis suspension	m	1
y_1	y-position of the front axis suspension	m	1
x_2	x-position of the rear axis suspension	m	1
y_2	y-position of the rear axis suspension	m	1
φ	(angular) orientation/direction of the center axis of the skateboard	rad	1
x_3	x-position of drivers mass m_3	m	1
y_3	y-position of drivers mass m_3	m	1
z_3	z-position of drivers mass m_3	m	1
θ	the bank of the board	rad	1
v_1	velocity of the front axis suspension in x-direction	m/s	1
w_1	velocity of the front axis suspension in y-direction	m/s	1
v_2	velocity of the rear axis suspension in x-direction	m/s	1
w_2	velocity of the rear axis suspension in y-direction	m/s	1
ω	angular velocity of the center axis of the skateboard	rad/s	1
v_3	velocity of drivers mass in x-direction m_3	m/s	1
w_3	velocity of drivers mass in y-direction m_3	m/s	1
u_3	velocity of drivers mass in z-direction m_3	m/s	1
ψ	angular banking velovity of the board	rad/s	1
λ	Lagrange-Multipliers for holonomic constraints	kg/s^2	5
μ	Lagrange-Multipliers for nonholonomic constraints	kg/s^2	2

Table 1: Unknown variables

variable	physical meaning	unit	dimension
α	steering angle α	rad	1

Table 2: Auxiliary variables

parameter	physical meaning	unit	dimension
m_1	mass of the mass point in the front suspension	kg	1
m_2	mass of the mass point in the rear suspension	kg	1
m_3	mass of the mass point for the driver	kg	1
J_1	(rotational) inertia of the skateboard for horizontal rotations	m kg	1
J_2	(rotational) inertia of the skateboard including driver for banking	m kg	1
d_1	damping coefficient of the mass point in the front suspension	kg/s	1
d_2	damping coefficient of the mass point in the rear suspension	kg/s	1
d_3	damping coefficient of the mass point for the driver	kg/s	1
d_φ	damping coefficient for the angular velocity of the center axis of the skateboard	m kg/s	1
d_θ	damping coefficient for the banking of the skateboard	kg	1
c	stiffness of the springs responsible for a vertical position of the driver	m kg/s	1
L_1	distance between rear and front suspension	m	1
L_3	distance of the mass point for the driver from the skateboard	m	1
$\mathfrak{g}$	gravitational acceleration	m/s^2	1
a	coefficient for the relation steering angle α of the wheele axes and the banking θ of the scate board	-	1

Table 3: Parameters

lose the contact to the surface, i.e., to the x-y-plane. The skateboard is constructed such that both axes are pivoted such that the axes are changing their relative direction denoted by the angle α with respect to the center axis of the board if the board banks. This yields a self stabilizing effect which is strongly influenced by the relation between α and θ, which is assumed to be

$$\alpha = a\theta$$

with the banking coefficient a.
Let us assume that the skateboarder is very unexperienced such that he is modeled just as the mass m_3 with position (x_3, y_3, z_3) which is located at a distance of L_3 perpendicular to the board as shown in the right of Figure 1.
If the position variables $p = \begin{bmatrix} x_1 & y_1 & x_2 & y_2 & \varphi & x_3 & y_3 & z_3 & \theta \end{bmatrix}^T$ could move freely in three dimensional space, the equations of motions would be given by

$$M\ddot{p} = f(p, \dot{p})$$

with

$$M = \begin{bmatrix} m_1 & & & & & & & & \\ & m_1 & & & & & & & \\ & & m_2 & & & & & & \\ & & & m_2 & & & & & \\ & & & & J_1 & & & & \\ & & & & & m_3 & & & \\ & & & & & & m_3 & & \\ & & & & & & & m_3 & \\ & & & & & & & & J_2 \end{bmatrix}, \; f(p, \dot{p}) = \begin{bmatrix} -d_1\dot{x}_1 \\ -d_1\dot{y}_1 \\ -d_2\dot{x}_2 \\ -d_2\dot{y}_2 \\ -d_\varphi\dot{\varphi} \\ -d_3\dot{x}_3 \\ -d_3\dot{y}_3 \\ -m_3\mathfrak{g} - d_3\dot{z}_3 \\ -c\theta - d_\theta\dot{\theta} \end{bmatrix},$$

where the stiffness c of the spring, the dampings d_1, d_2, d_3, d_φ, d_θ, and the gravitational acceleration $\mathfrak{g}$ are given. Furthermore, J_1 and J_2 denote the inertia of the board with respect to the rotations φ and θ, respectively. But obviously the positions are restricted in its choice by holonomic constraints $0 = g(p)$ (also called holonomic constraints on position level) with

$$\begin{aligned} g_1 &= x_2 + L_1\cos(\varphi) - x_1, \\ g_2 &= y_2 + L_1\sin(\varphi) - y_1, \\ g_3 &= (x_1 + x_2)/2 + L_3\cos(\varphi - \pi/2)\sin(\theta) - x_3, \\ g_4 &= (y_1 + y_2)/2 + L_3\sin(\varphi - \pi/2)\sin(\theta) - y_3, \\ g_5 &= L_3\cos(\theta) - z_3, \end{aligned}$$

where L_1 denotes the distance between the center of the axes of the skateboard and L_3 denotes the distance between the mass m_3 and the center of the board. From the holonomic constraints we get the holonomic constraint matrix $G(p) = \frac{\partial}{\partial p} g(p)$

$$G(p) = \begin{bmatrix} -1 & 0 & 1 & 0 & -L_1\sin(\varphi) & 0 & 0 & 0 & 0 \\ 0 & -1 & 0 & 1 & L_1\cos(\varphi) & 0 & 0 & 0 & 0 \\ 1/2 & 0 & 1/2 & 0 & -L_3\sin(\varphi_\perp)\sin(\theta) & -1 & 0 & 0 & L_3\cos(\varphi_\perp)\cos(\theta) \\ 0 & 1/2 & 0 & 1/2 & L_3\cos(\varphi_\perp)\sin(\theta) & 0 & -1 & 0 & L_3\sin(\varphi_\perp)\cos(\theta) \\ 0 & 0 & 0 & 0 & 0 & 0 & 0 & -1 & -L_3\sin(\theta) \end{bmatrix}$$

with $\varphi_\perp = \varphi - \pi/2$.
Furthermore, let us assume that the skateboard is not allowed to slide on the surface. In particular, this means that the motion of the wheels is perpendicular to its axes. This leads to the nonholonomic constraints $0 = \breve{h}(p, \dot{p})$ (also called nonholonomic constraints on velocity level) with

$$\begin{aligned} \breve{h}_1 &= \begin{bmatrix} x_1 - x_2 & y_1 - y_2 \end{bmatrix} \begin{bmatrix} \cos(\pi/2 - \alpha) & \sin(\pi/2 - \alpha) \\ -\sin(\pi/2 - \alpha) & \cos(\pi/2 - \alpha) \end{bmatrix} \begin{bmatrix} \dot{x}_1 \\ \dot{y}_1 \end{bmatrix}, \\ \breve{h}_2 &= \begin{bmatrix} x_1 - x_2 & y_1 - y_2 \end{bmatrix} \begin{bmatrix} \cos(\pi/2 + \alpha) & \sin(\pi/2 + \alpha) \\ -\sin(\pi/2 + \alpha) & \cos(\pi/2 + \alpha) \end{bmatrix} \begin{bmatrix} \dot{x}_2 \\ \dot{y}_2 \end{bmatrix}. \end{aligned}$$

They have the form $\breve{h}(p, \dot{p}) = H(p)\dot{p}$ with the nonholonomic constraint matrix $H(p)$ with

$$H^T(p) = \begin{bmatrix} \Delta x\cos(\pi/2 - \alpha) - \Delta y\sin(\pi/2 - \alpha) & 0 \\ \Delta x\sin(\pi/2 - \alpha) + \Delta y\cos(\pi/2 - \alpha) & 0 \\ 0 & \Delta x\cos(\pi/2 + \alpha) - \Delta y\sin(\pi/2 + \alpha) \\ 0 & \Delta x\sin(\pi/2 + \alpha) + \Delta y\cos(\pi/2 + \alpha) \\ 0 & 0 \\ 0 & 0 \\ 0 & 0 \\ 0 & 0 \\ 0 & 0 \end{bmatrix}$$

with $\Delta x = (x_1 - x_2)$ and $\Delta y = (y_1 - y_2)$. Hence, the equations of motion for the skateboard have the form

$$\begin{aligned} \dot{p} &= v, \\ M\dot{v} &= f(p,v) - G^T(p)\lambda - H^T(p)\mu, \\ 0 &= g(p), \\ 0 &= H(p)v \end{aligned}$$

with the *kinematic equations of motion* (1a), the *dynamic equations of motion* (1b), the *holonomic constraints* (1c), and the *nonholonomic constraints* (1d). Furthermore, we have introduced the vector of velocities $v = \dot{p}$ with $v = \begin{bmatrix} v_1 & w_1 & v_2 & w_2 & \omega & v_3 & w_3 & u_3 & \psi \end{bmatrix}^T$ and we have the *holonomic constraint force* $G^T\lambda$ and the *nonholonomic constraint force* $H^T\mu$ and their associated *Lagrange multipliers* λ and μ.
The unknown and auxiliary variables as well as the model parameters are listed in Tables 1 and 2, and within the scenarios below together with its physical meaning and units.

2.1.3 Analysis of the Model Equations

Hidden Constraints In the following we use the comma-notation for expressing partial derivatives, e.g., $g_{,p}(p) = \frac{\partial}{\partial p} g(p)$ or $(G(p)v)_{,p} = \frac{\partial}{\partial p}(G(p)v)$.
The solution of the model equations is restricted by so called *hidden constraints* which, in particular, are responsible for the diffuculties in the numerical treatement. In particlar, as hidden constraints we have

$$0 = G(p)v, \tag{2a}$$

the *holonomic constraints of velocity level* obtained from the total time derivative of the holonomic constraints (1c), where the derivatives $\dot{p}$ are replaced by (1a). Further hidden constraints are

$$\begin{aligned} 0 &= (G(p)v)_{,p}v + G(p)M^{-1}(f(p,v) - G^T(p)\lambda - H^T(p)\mu), && \text{(2b)} \\ 0 &= (H(p)v)_{,p}v + H(p)M^{-1}(f(p,v) - G^T(p)\lambda - H^T(p)\mu) && \text{(2c)} \end{aligned}$$

the *holonomic constraints of acceleration level* and the *nonholonomic constraints of acceleration level*, respectively. These are obtained from the total time derivative of the holonomic constraints on velocity level (2a) and the total time derivative of the nonholonomic constraints (1d), where the derivatives $\dot{p}$ and $\dot{v}$ are replaced by (1a) and (1b).

2.1.4 Regularizations and used Formulations

For the numerical treatment we will use the following formulations.

d-index 2 formulation (EoM1) The d-index 2 formulation has the form

$$\begin{aligned} \dot{p} &= v, && \text{(3a)} \\ M\dot{v} &= f(p,v) - G^T(p)\lambda - H^T(p)\mu, && \text{(3b)} \\ 0 &= G(p)v, && \text{(3c)} \\ 0 &= H(p)v && \text{(3d)} \end{aligned}$$

and belongs to the classical index reduction, where in the model equations (1) the holonomic constraints (1c) are replaced by the holonomic constraints on velocity level (2a). This formulation has d-index 2, s-index 1, and maximal constraint level 1. Furthermore, in its numerical treatement slight instabilities due to the higher index and linear drift from the holonomic constraints (1c) is expected due to the lost of these constraints on position level. For more details we refer to [2, 6, 7].

d-index 1 formulation (EoM0) The d-index 1 formulation has the form

$$\begin{aligned} \dot{p} &= v, && \text{(4a)} \\ M\dot{v} &= f(p,v) - G^T(p)\lambda - H^T(p)\mu, && \text{(4b)} \\ 0 &= (G(p)v)_{,p}v + G(p)M^{-1}(f(p,v) - G^T(p)\lambda - H^T(p)\mu), && \text{(4c)} \\ 0 &= (H(p)v)_{,p}v + H(p)M^{-1}(f(p,v) - G^T(p)\lambda - H^T(p)\mu) && \text{(4d)} \end{aligned}$$

and belongs to the classical index reduction, where in the model equations (1) the holonomic constraints (1c) are replaced by holonomic constraints on acceleration level (2b) and where the nonholonomic constraints (1d) are replaced by the nonholonomic constraints on acceleration level (2c). This formulation has d-index 1, s-index 0, and maximal constraint level 0. Furthermore, in its numerical treatement no instabilities but quadratic drift from the holonomic constraints (1c) and linear drift from the nonholonomic constraints (1d) is expected due to the lost of the constraints on position level and velocity level. For more details we refer to [2, 6, 7].

overdetermined c-level 1 formulation (oEoM1) The overdetermined c-level 1 formulation has the form

$$\begin{aligned} \dot{p} &= v, && \text{(5a)}\\ M\dot{v} &= f(p,v) - G^T(p)\lambda - H^T(p)\mu, && \text{(5b)}\\ 0 &= g(p), && \text{(5c)}\\ 0 &= G(p)v, && \text{(5d)}\\ 0 &= H(p)v, && \text{(5e)} \end{aligned}$$

where the holonomic constraints on velocity level (2a) are added to the model equations (1). This formulation has s-index 1, and maximal constraint level 1 while the d-index is not defined. Furthermore, the direct numerical integration needs adapted numerical methods suited for overdetermined DAEs. In its numerical treatement slight instabilities due to the higher c-level but no drift are expected. For more details we refer to [7].

overdetermined c-level 0 formulation (oEoM0) The overdetermined c-level 0 formulation has the form

$$\begin{aligned} \dot{p} &= v, && \text{(6a)}\\ M\dot{v} &= f(p,v) - G^T(p)\lambda - H^T(p)\mu, && \text{(6b)}\\ 0 &= g(p), && \text{(6c)}\\ 0 &= G(p)v, && \text{(6d)}\\ 0 &= H(p)v, && \text{(6e)}\\ 0 &= (G(p)v)_{,p}v + G(p)M^{-1}(f(p,v) - G^T(p)\lambda - H^T(p)\mu), && \text{(6f)}\\ 0 &= (H(p)v)_{,p}v + H(p)M^{-1}(f(p,v) - G^T(p)\lambda - H^T(p)\mu), && \text{(6g)} \end{aligned}$$

where the holonomic constraints on velocity level (2a) and on acceleration level (2b) as well as the nonholonomic constraints on acceleration level (2c) are added to the model equations (1). This formulation has s-index 1, and maximal constraint level 0 while the d-index is not defined. Furthermore, the direct numerical integration needs adapted numerical methods suited for overdetermined DAEs. In its numerical treatement no instabilities and no drift are expected. For more details we refer to [7].

Gear-Gupta-Leimkuhler formulation (GGL) The Gear-Gupta-Leimkuhler formulation has the form

$$\begin{aligned} \dot{p} &= v - G^T(p)\eta, && \text{(7a)}\\ M\dot{v} &= f(p,v) - G^T(p)\lambda - H^T(p)\mu, && \text{(7b)}\\ 0 &= g(p), && \text{(7c)}\\ 0 &= G(p)v, && \text{(7d)}\\ 0 &= H(p)v, && \text{(7e)} \end{aligned}$$

where the holonomic constraints on velocity level (2a) are added to the model equations (1) and additional Lagrange multipliers η with $\eta(t_0) = 0 \in \mathbb{R}^2$ are introduced. Therefore, the number of unknowns is increased. This formulation has d-index 2, s-index 1, and maximal constraint level 1. In its numerical treatement slight instabilities due to the higher index but no drift are expected. For more details we refer to [4].

2.2 Numerical Results

For the numerical computations we use the following solvers combined with the original model equations (1) (denoted by (EoM)) and the regularized formulations presented in Section 2.1.4.

`DASSL` (Version from 24.Jun.1991) [1] is suited for nonlinear DAEs of d-index 1 and uses BDF-methods of order 1 up to 5 as discretization scheme.

`GEOMS` (Version 1.3 from 17.Nov.2014) [7, 8] is suited for equations of motion for multibody systems and its regularizations based on overdetermined formulations and uses the Runge-Kutta method of type RADAU IIa of order 5 as discretization scheme.

`ODASSL` (Version from 03.Jan.1990) [2, 3] is suited for (possibly overdetermined) nonlinear DAEs with maximal c-level 0 and uses an adaption of the BDF-methods of order 1 up to 5 as discretization scheme.

`RADAU5` (Version with small correction from April 14, 2000) [5, 6] is suited for quasi-linear DAEs with constant leading matrix up to d-index 2 and for Hessenberg systems up to d-index 3 and uses the Runge-Kutta method of type RADAU IIa of order 5 as discretization scheme.

The numerical integrations are done on an AMD Phenom(tm) II X6 1090T, 3210 MHz.

2.2.1 Scenario 01

The equations of motion are given in (1). First, let us simulate the motion of the skater on $\mathbb{I} = [0\text{s}, 100\text{s}]$

masses	$m_1 = 1 \quad m_2 = 1 \quad m_3 = 80$
inertias	$J_1 = 0.001 \quad J_2 = 0.001$
lengths	$L_1 = 0.5 \quad L_3 = 1.5$
stiffness	$c = 0$
dampings	$d_1 = d_2 = d_3 = d_\varphi = d_\theta = 0.01$
gravitational acceleration	$\mathfrak{g} = 9.81$
banking coefficient	$a = 11.0$

Table 4: Secenario 01: Parameters

with the parameter as depicted in Table 4 and the initial values

$$
\begin{array}{rclrclrcl}
x_1(t_0) &=& 0.25, & \dot{x}_1(t_0) &=& 0.5, & \lambda_1(t_0) &=& 0,\\
y_1(t_0) &=& 0, & \dot{y}_1(t_0) &=& 0, & \lambda_2(t_0) &=& 0.44e-04,\\
x_2(t_0) &=& -0.25, & \dot{x}_2(t_0) &=& 0.5, & \lambda_3(t_0) &=& -0.9634e-03,\\
y_2(t_0) &=& 0, & \dot{y}_2(t_0) &=& 0, & \lambda_4(t_0) &=& 0.6667e-06,\\
\varphi(t_0) &=& 0, & \dot{\varphi}(t_0) &=& 0, & \lambda_5(t_0) &=& 784.8,\\
x_3(t_0) &=& 0, & \dot{x}_3(t_0) &=& 0.5, & \mu_1(t_0) &=& 0.01109,\\
y_3(t_0) &=& 0, & \dot{y}_3(t_0) &=& -0.0015, & \mu_2(t_0) &=& -0.01109,\\
z_3(t_0) &=& 1.5, & \dot{z}_3(t_0) &=& 0, & & & \\
\theta(t_0) &=& 0, & \dot{\theta}(t_0) &=& 0.001. & & &
\end{array}
$$

Reference Solution For reasons of comparisons of the accuracy a reference solution is needed since an analytical solution is not available. Therefore, we use the numerical solution obtained with `RADAU5`(GGL) for a prescribed tolerance of `RTOL`=`ATOL`=10^{-15} as reference solution which is illustrated in Figures 2, 3, and 4.
In Table 5 the values of the reference solution at the final time t_f is listed.

Numerical Solution The driver subroutines for the used solver-formulation combinations are available on the webpage `http://www3.math.tu-berlin.de/multiphysics/Examples/M007_SkateBoard/`.
The numerical solutions with the different solver-formulation combinations for p are shown in Figure 5. It seems that all solutions are of similar quality except the solutions based on the s-index-0 formulation, i.e., `DASSL`(EoM0) and `RADAU5`(EoM0), in the component p_8. In Figure 6 the obtained accuracy by a prescribed tolerance of `RTOL`=`ATOL`=10^{-7} is illustrated and it is obvious that numerical solutions `DASSL`(EoM0) and `RADAU5`(EoM0) are not very accurate as mentioned. The accuracy of the numerical solutions is compared with the numerical solution `RADAU5`(GGL) obtained with a prescribed tolerance `RTOL`=`ATOL`=10^{-15}.

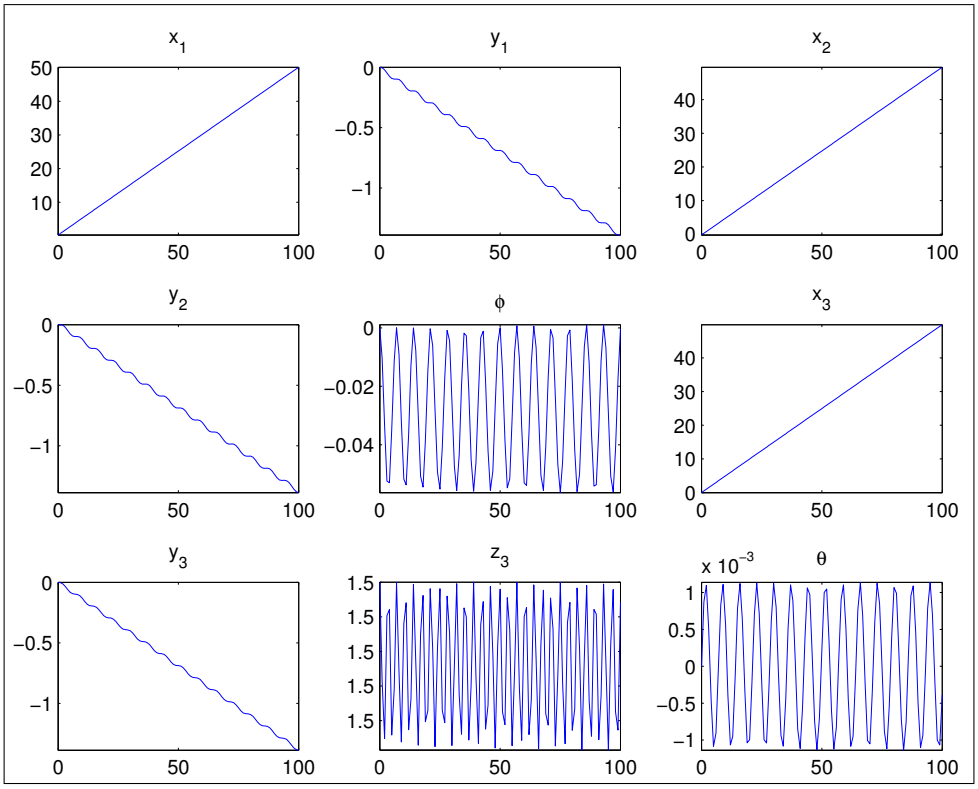

Figure 2: Scenario 01: Reference solution for the positions p with RADAU5(GGL) and RTOL=ATOL=10^{-15}

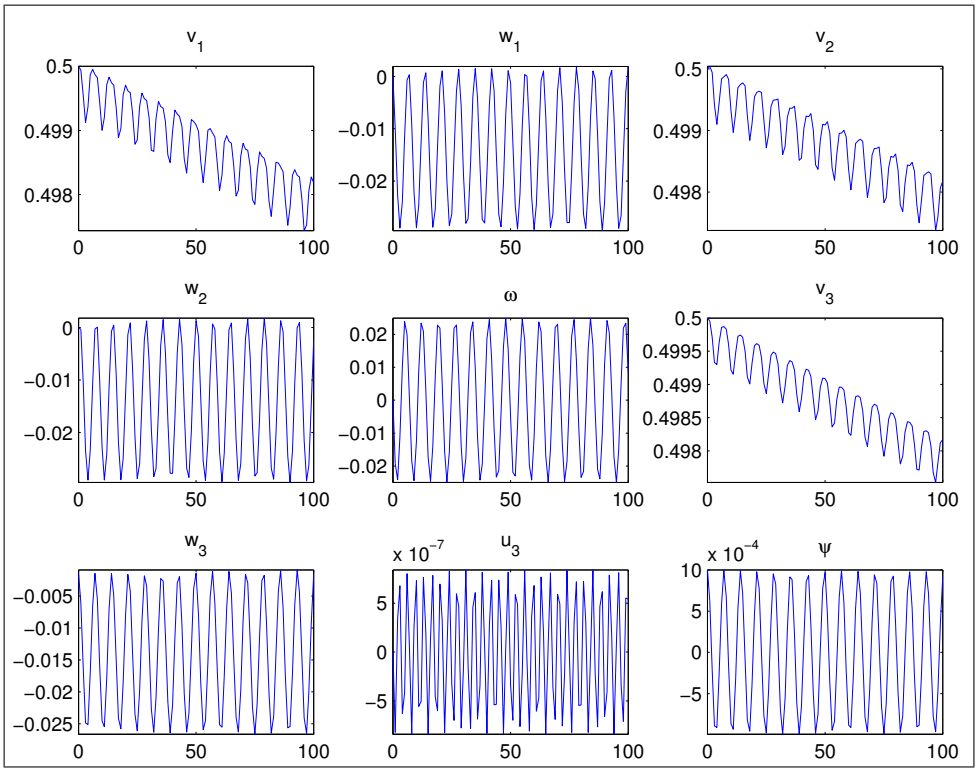

Figure 3: Scenario 01: Reference solution for the velocities v with RADAU5(GGL) and RTOL=ATOL=10^{-15}

In Figures 7 and 8 the efficiency of the solvers is illustrated. Obviously, the numerical solutions GEOMS(oEoM1) and RADAU5(EoM1) are obtained in a very efficient way for all prescribed tolerances RTOL=ATOL=10^i with $i = -3, ..., -12$. For large prescribed tolerances, i.e., RTOL = ATOL = 10^i with

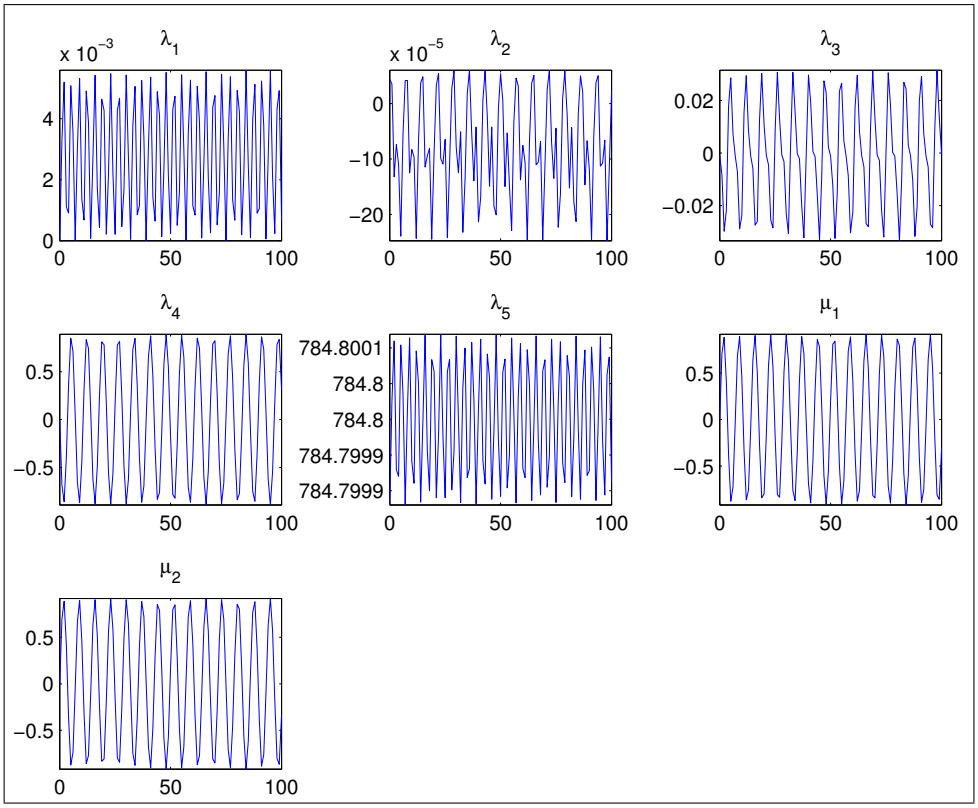

Figure 4: Scenario 01: Reference solution for the Lagrange multipliers λ and μ with RADAU5(GGL) and RTOL=ATOL=10^{-15}

$x_1(t_f) =$	0.5013234894447380E+02	$v_1(t_f) =$	0.4981812182203535E+00
$y_1(t_f) =$	-0.1387919293879772E+01	$w_1(t_f) =$	0.1943122219849499E-02
$x_2(t_f) =$	0.4963234898565554E+02	$v_1(t_f) =$	0.4981794767995704E+00
$y_2(t_f) =$	-0.1387716361047717E+01	$w_1(t_f) =$	-0.2347510848334840E-02
$\varphi(t_f) =$	-0.4058656752523516E-03	$\omega(t_f) =$	0.8581266843151610E-02
$x_3(t_f) =$	0.4988234920339701E+02	$v_1(t_f) =$	0.4981747469843218E+00
$y_3(t_f) =$	-0.1387230607744375E+01	$w_1(t_f) =$	-0.1585498461601943E-02
$z_3(t_f) =$	0.1499999885057644E+01	$u_1(t_f) =$	0.5415365801650969E-06
$\theta(t_f) =$	-0.3914798551564864E-03	$\psi(t_f) =$	0.9222042749912872E-03

$\lambda_1(t_f) =$	0.6615310466783268E-03
$\lambda_1(t_f) =$	0.2200517767255407E-04
$\lambda_1(t_f) =$	-0.7230900547208262E-03
$\lambda_1(t_f) =$	0.3072344981071227E+00
$\lambda_1(t_f) =$	0.7847999115540488E+03
$\mu_1(t_f) =$	-0.3056388253068474E+00
$\mu_1(t_f) =$	-0.3259354647014435E+00

Table 5: Scenario 01: Reference solution at the final time point $t_f = 100$s for scenario 01 with RADAU5(GGL) and RTOL=ATOL=10^{-15}.

$i = -3, ..., -7$ the numerical results GEOMS(oEoM0) are not obtained very efficiently, but for smaller tolerances, the efficiency of GEOMS is growing and, in particular, it is more efficient than RADAU5 with use of the Gear-Gupta-Leimkuhler formulation. The efficiency of DASSL as well as of ODASSL is slightly reduced and the best obtained accuracy, approximately 10^{-6} and 10^{-7}, respectively, is not as good as the one of the other numerical solutions, except RADAU5(EoM0). The efficiency obtaining the results RADAU5(EoM0) is out of interest.

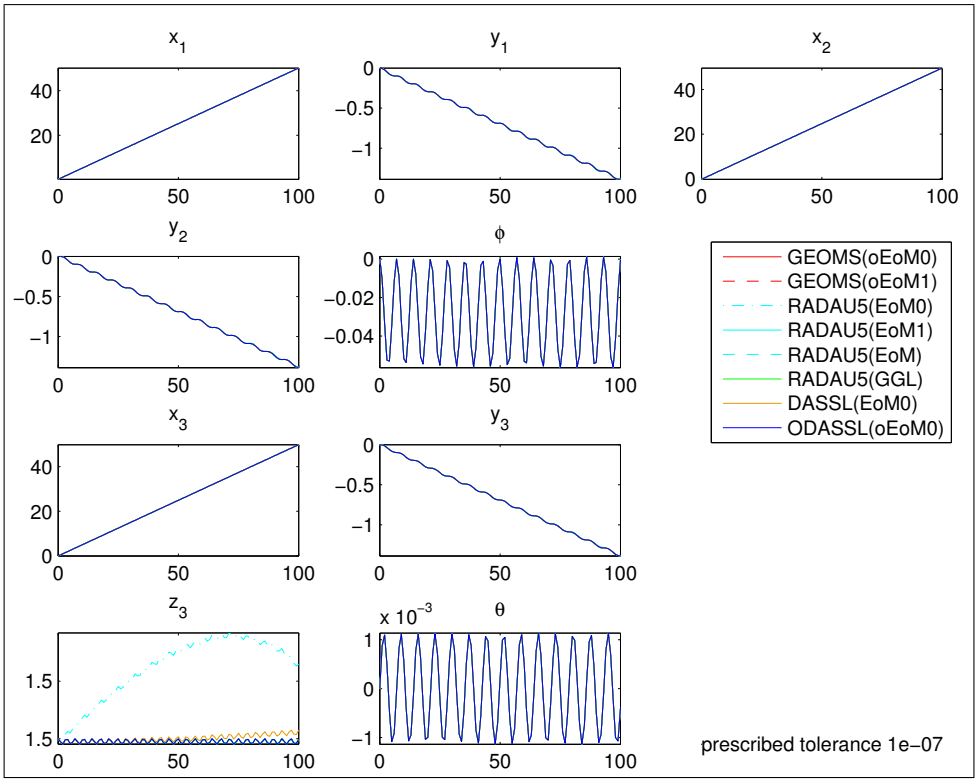

Figure 5: Scenario 01: Numerical solutions with the tolerance RTOL=ATOL=10^{-7}.

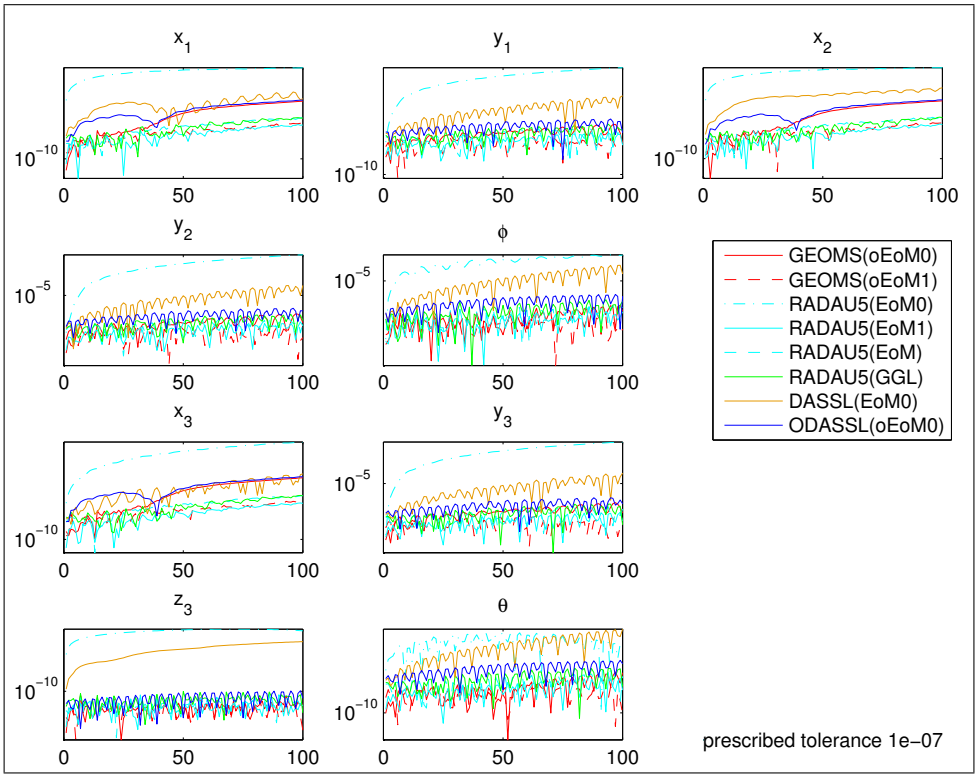

Figure 6: Scenario 01: Numerical error with the tolerance RTOL=ATOL=10^{-7}.

2.2.2 Scenario 02

In the following we will change the parameter of the model of the skateboard as shown in Table 6.

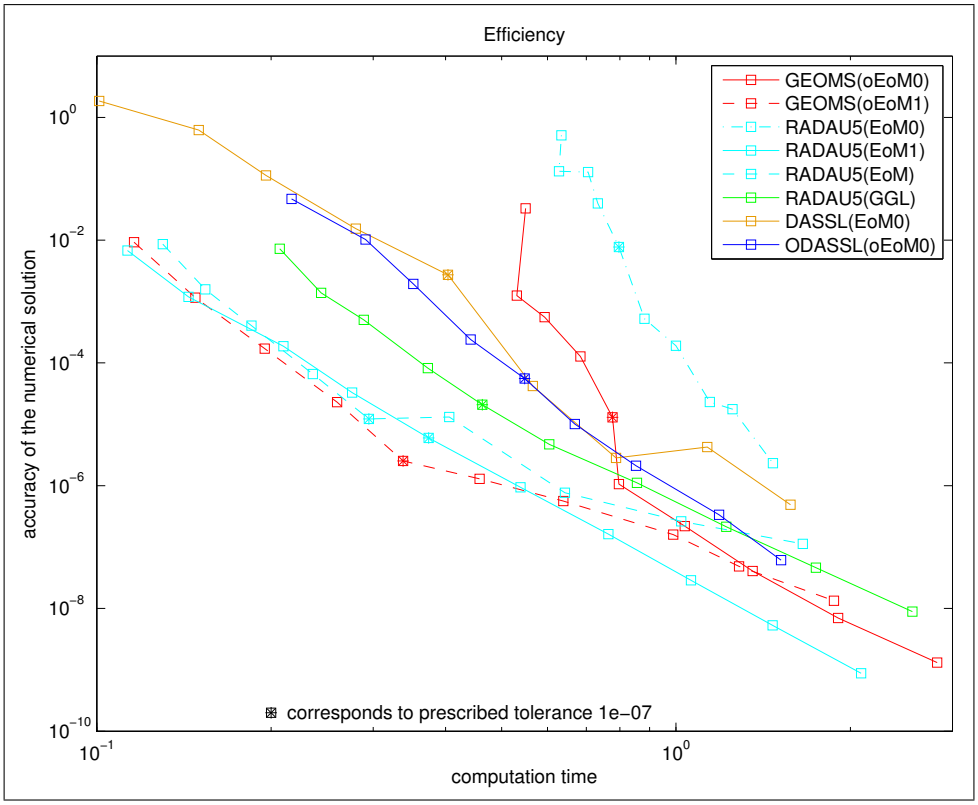

Figure 7: Scenario 01: Efficiency.

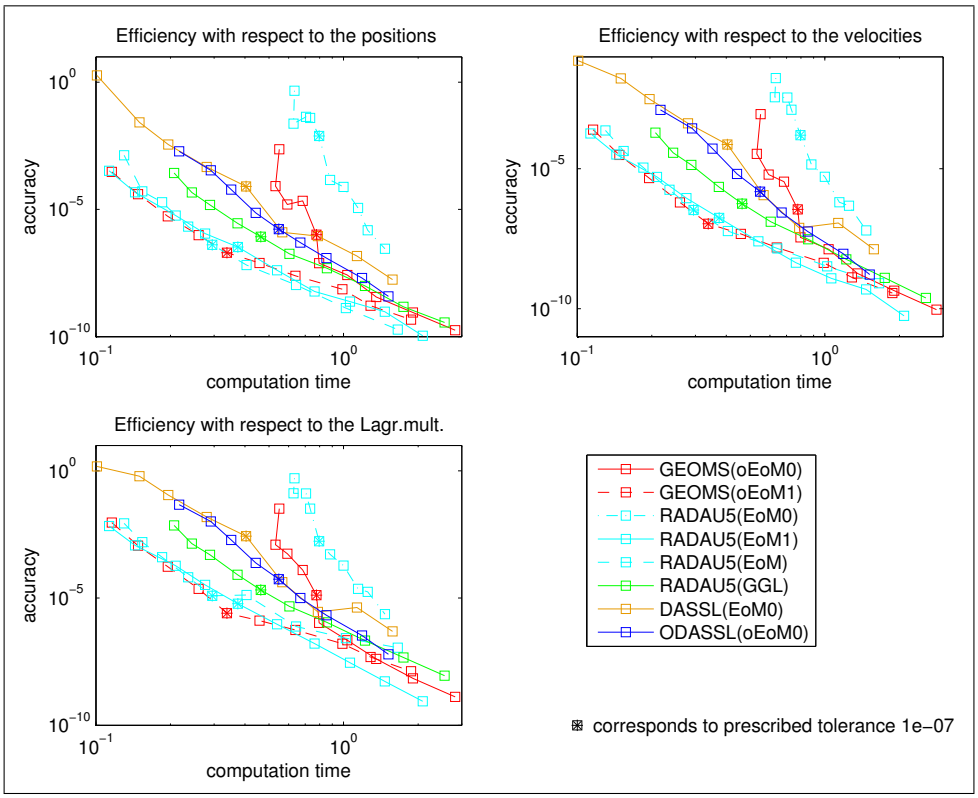

Figure 8: Scenario 01: Efficiency with respect to positions, velocities, and Lagrange multipliers.

Furthermore, we will simulate the motion of the skater on $\mathbb{I} = [0\text{s}, 10\text{s}]$ with use the initial values

$$\begin{array}{lllllllll}
x_1(t_0) & = & 0.25, & \dot{x}_1(t_0) & = & 5, & \lambda_1(t_0) & = & 0, \\
y_1(t_0) & = & 0, & \dot{y}_1(t_0) & = & 0, & \lambda_2(t_0) & = & 0.044, \\
x_2(t_0) & = & -0.25, & \dot{x}_2(t_0) & = & 5, & \lambda_3(t_0) & = & -0.04817, \\
y_2(t_0) & = & 0, & \dot{y}_2(t_0) & = & 0, & \lambda_4(t_0) & = & 0.0003333, \\
\varphi(t_0) & = & 0, & \dot{\varphi}(t_0) & = & 0, & \lambda_5(t_0) & = & 783.6, \\
x_3(t_0) & = & 0, & \dot{x}_3(t_0) & = & 5, & \mu_1(t_0) & = & 11.09,
\end{array}$$

masses	$m_1 = 1 \quad m_2 = 1 \quad m_3 = 80$
inertias	$J_1 = 0.001 \quad J_2 = 0.001$
lengths	$L_1 = 0.5 \quad L_3 = 1.5$
stiffness	$c = 1$
dampings	$d_1 = d_2 = d_3 = d_\varphi = d_\theta = 0.005$
gravitational acceleration	$\mathfrak{g} = 9.81$
banking coefficient	$a = 11.0$

Table 6: Scenario 02: Used parameters and initial values

In particular, mainly we did introduce a stiffness c and reduced the damping d_1, d_2, d_3, d_φ, d_θ of the system. To compensate these changes, we increased the initial velocity of the skateboard.

Reference Solution For reasons of comparisons of the accuracy a reference solution is needed since an analytical solution is not available. Since the best result we obtained for `RADAU5`(GGL) was for `RTOL`=`ATOL`=10^{-11}, here we used the numerical solution obtained with `GEOMS`(oEoM0) for a prescribed tolerance of `RTOL`=`ATOL`=10^{-15} as reference solution and as illustrated in Figures 9, 10, and 11.

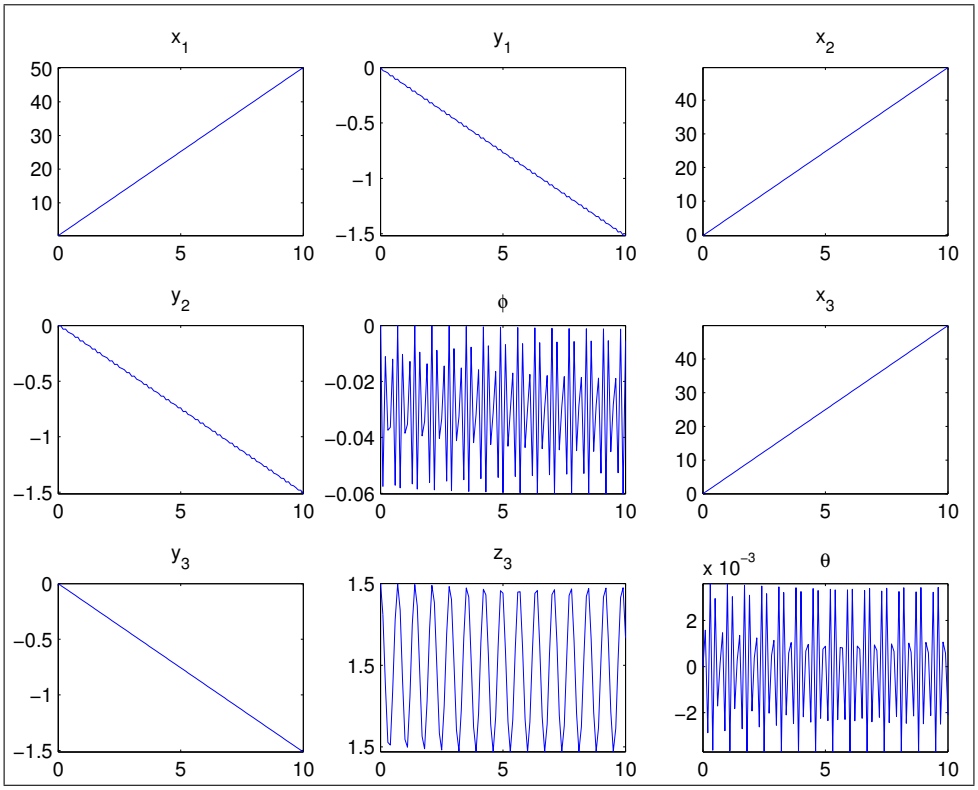

Figure 9: Scenario 02: Reference solution for the positions p with `GEOMS`(oEoM0) and `RTOL`=`ATOL`=10^{-15}

In Table 7 the values of the reference solution at the final time t_f is listed.

Numerical solution The driver subroutines for the used solver-formulation combinations are available on the webpage `http://www3.math.tu-berlin.de/multiphysics/Examples/M007_SkateBoard/`.
In Figure 12 we have illustrated the solution of the numerical integration by use of the different solver-formulation combinations with a prescribed tolerance `RTOL`=`ATOL`=10^{-7}. In comparison to the first scenario the oscillating motion is increased, i.e., the frequence, as we can see, in particular, in the solution component φ and θ. Analogously to the first test scenario, the numerical solutions seem to be of comparable accuracy, except the numerical solutions `RADAU5`(EoM0) with a visible deviation. The absolute error of the position components is illustrated in Figure 13. Apart from the numerical results `RADAU5`(EoM0) and `DASSL`(EoM0), all numerical results satisfy the prescribed tolerance.

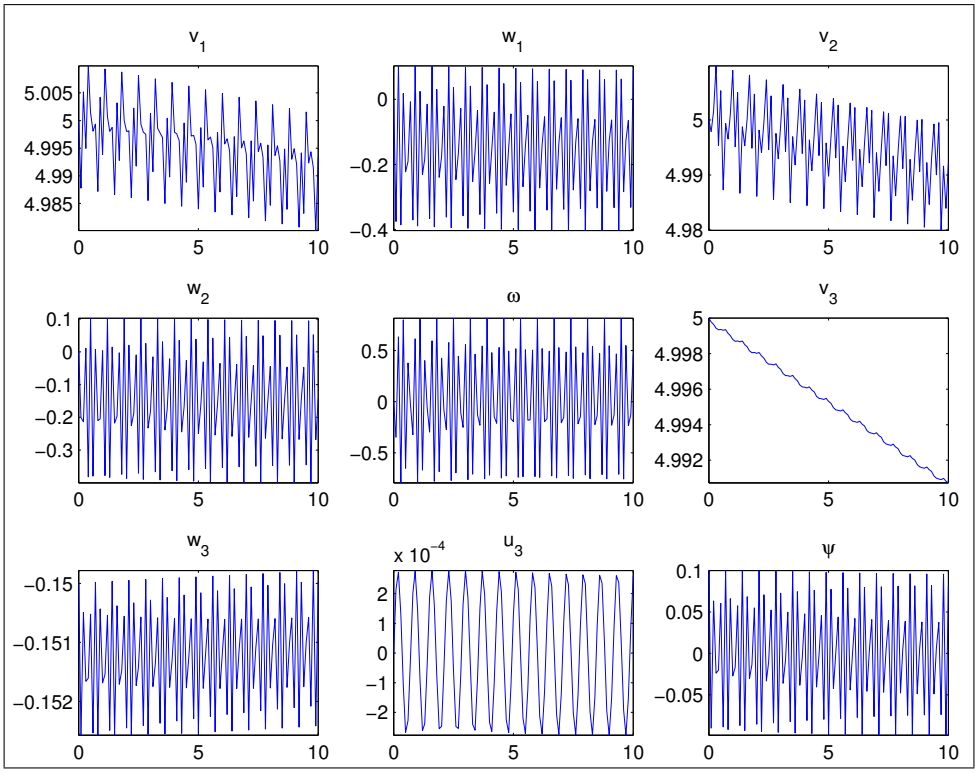

Figure 10: Scenario 02: Reference solution for the velocities v with `GEOMS`(oEoM0) and `RTOL`=`ATOL`=10^{-15}

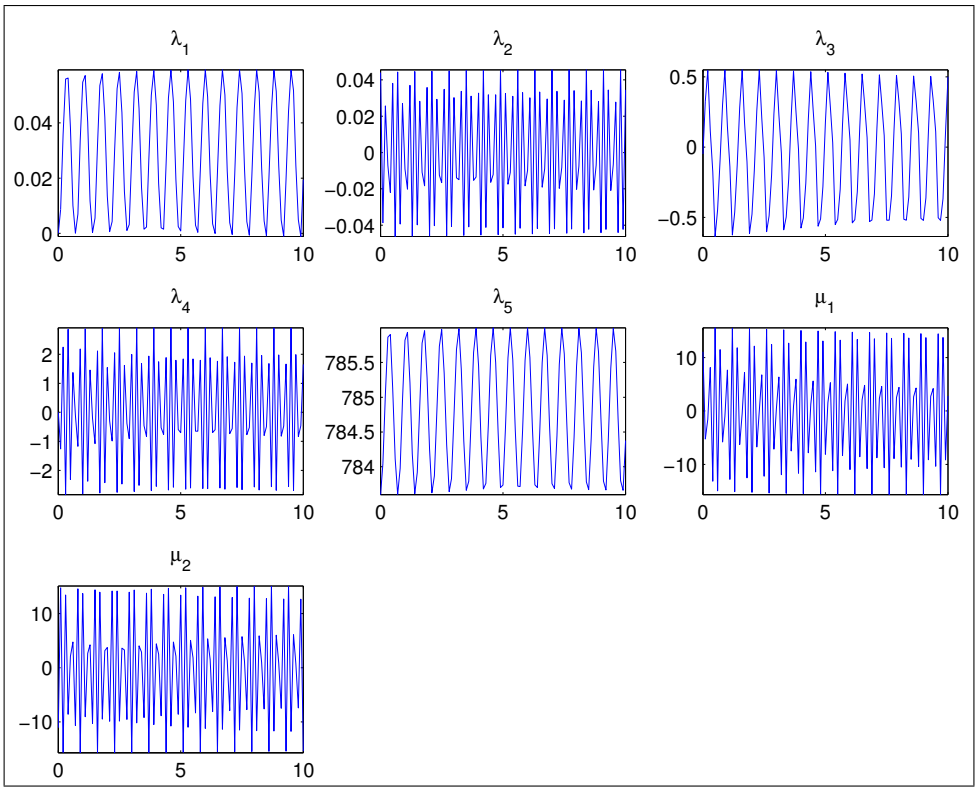

Figure 11: Scenario 02: Reference solution for the Lagrange multipliers λ and μ with `GEOMS`(oEoM0) and `RTOL`=`ATOL`=10^{-15}

In Figures 14 and 15, the efficiency of the several used numerical integrations is shown. Again the efficiency behavior for obtaining the numerical results `RADAU5`(EoM0) is not acceptable and even the nu-

$x_1(t_f) =$	0.5020238015216194E+02	$v_1(t_f) =$	0.4993477042271962E+01
$y_1(t_f) =$	-0.1516634200713534E+01	$w_1(t_f) =$	0.8917463647163969E-01
$x_2(t_f) =$	0.4970238734339254E+02	$v_1(t_f) =$	0.4992233247991682E+01
$y_2(t_f) =$	-0.1513952563361336E+01	$w_1(t_f) =$	-0.1427315141565594E+00
$\varphi(t_f) =$	-0.5363300416906395E-02	$\omega(t_f) =$	0.4638189721147709E+00
$x_3(t_f) =$	0.4995240072957007E+02	$v_1(t_f) =$	0.4990725873122798E+01
$y_3(t_f) =$	-0.1512127117109360E+01	$w_1(t_f) =$	-0.1499581293996815E+00
$z_3(t_f) =$	0.1499996658155619E+01	$u_1(t_f) =$	0.2600377079494569E-03
$\theta(t_f) =$	-0.2110875212545647E-02	$\psi(t_f) =$	0.8212640883632240E-01

$\lambda_1(t_f) =$	0.1941019588068094E-01
$\lambda_1(t_f) =$	0.3451313918161713E-01
$\lambda_1(t_f) =$	0.5015905632315704E+00
$\lambda_1(t_f) =$	0.1652946577846409E+01
$\lambda_1(t_f) =$	0.7843780909001475E+03
$\mu_1(t_f) =$	0.2815275745455883E+01
$\mu_1(t_f) =$	-0.1539314921877599E+02

Table 7: Scenario 02: Reference solution at the final time point $t_f = 10$s with `GEOMS`(oEoM0) and `RTOL`=`ATOL`=10^{-15}

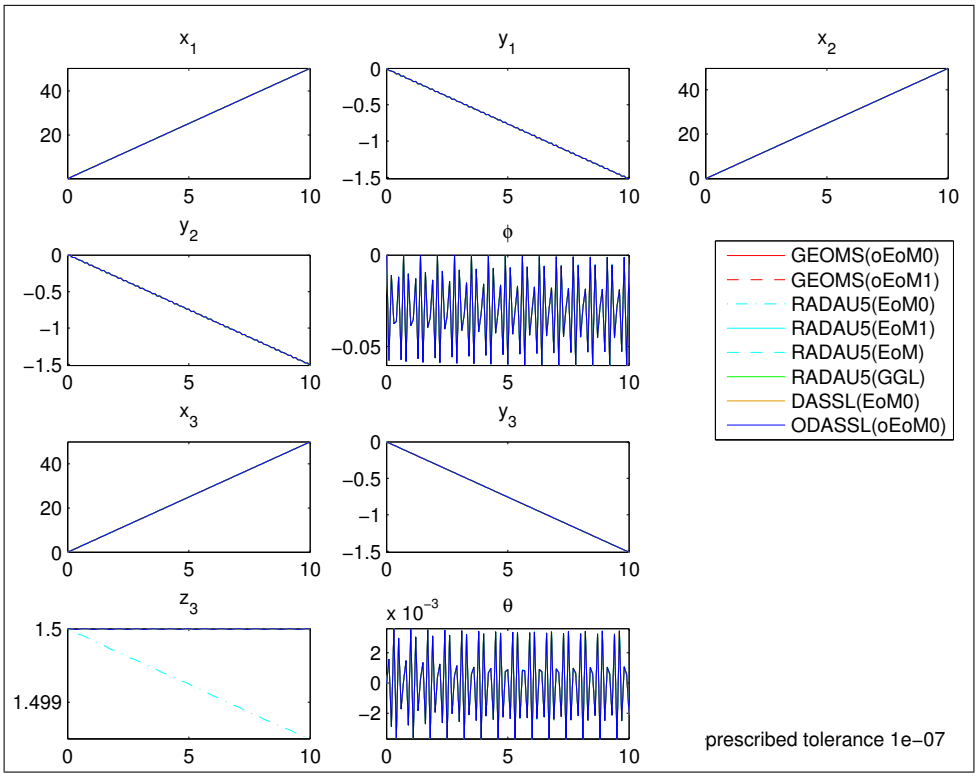

Figure 12: Scenario 02: Numerical solutions with the tolerance `RTOL`=`ATOL`=10^{-7}.

merical results `RADAU5`(EoM), too. Furthermore, the comparison of the efficiency of the several numerical integration methods has to be partitioned into two accuracy ranges. First, for an obtained accuracy in $[10^2, 10^{-4}]$ the results `RADAU5`(EoM1) and `GEOMS`(oEoM1) are obtained in a very efficient way closely followed by `RADAU5`(GGL), `DASSL`(EoM0), and `ODASSL`(oEoM0). Secondly, for an obtained accuracy in $[10^{-4}, 10^{-8}]$ the results `ODASSL`(oEoM0) are obtained in a very efficient way followed by `GEOMS`(oEoM1), `GEOMS`(oEoM0), and `RADAU5`(GGL) while only the results `GEOMS`(oEoM0) does reach a accuracy in the range of approximately $[10^{-6}, 10^{-8}]$.

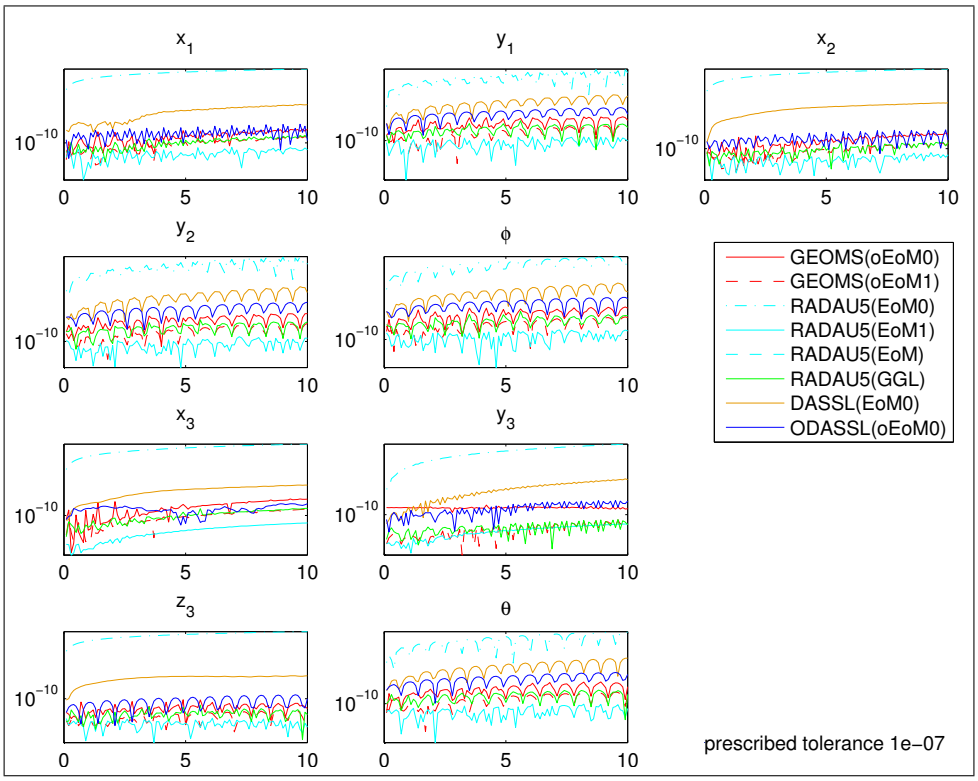

Figure 13: Scenario 01: Numerical error with the tolerance RTOL=ATOL=10^{-7}.

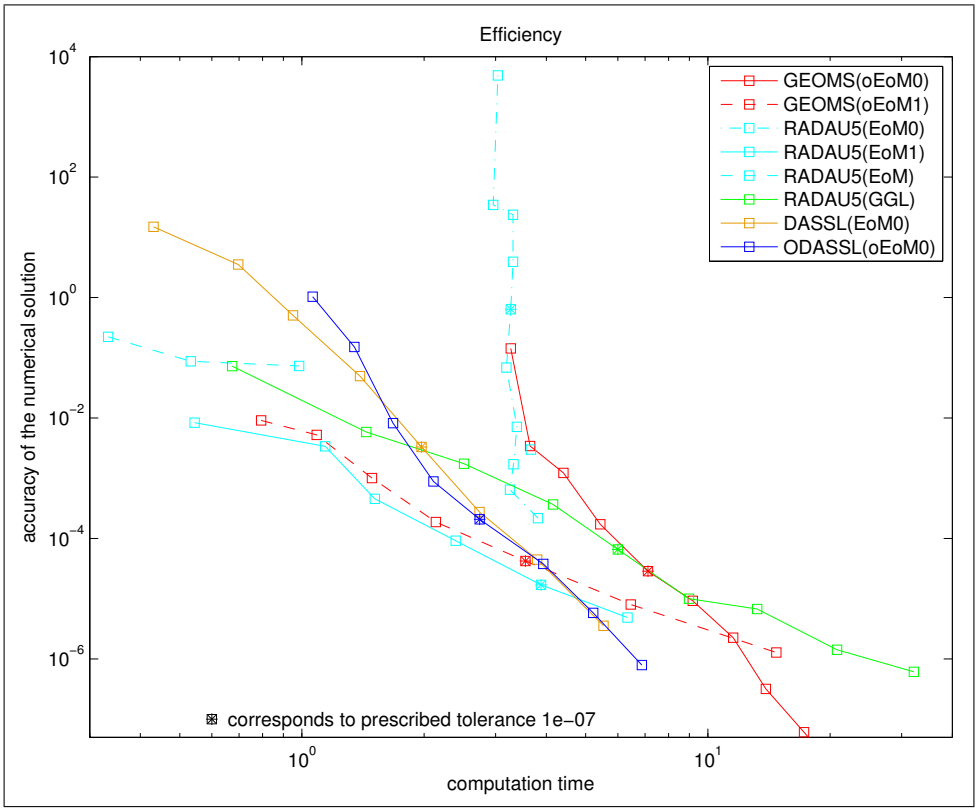

Figure 14: Scenario 01: Efficiency.

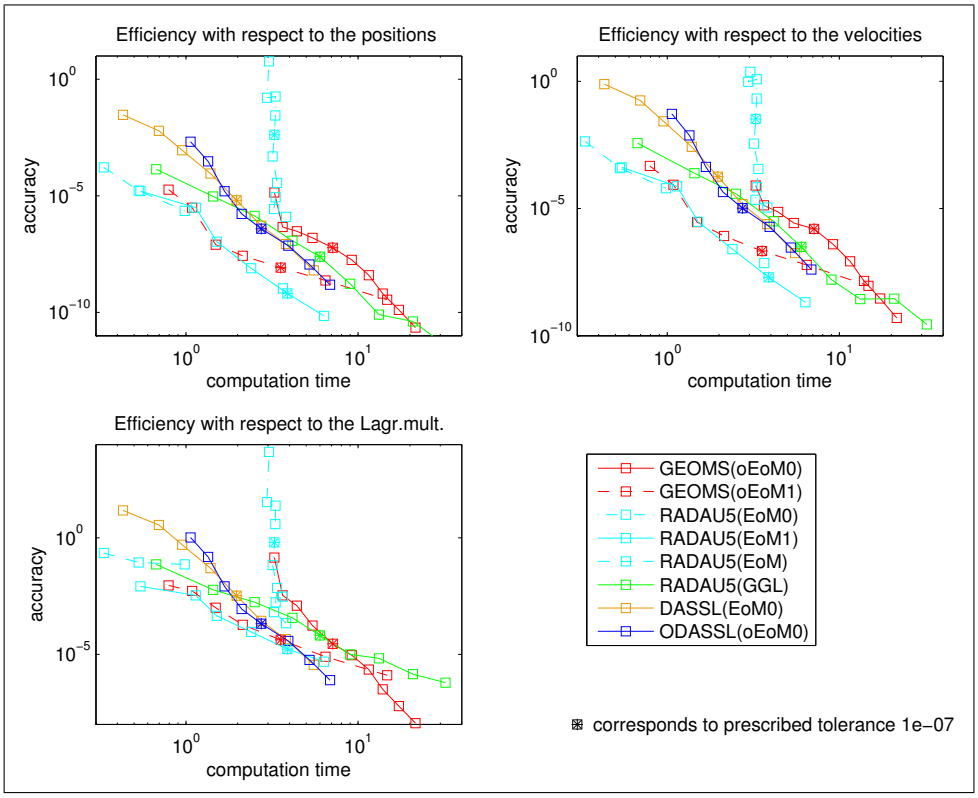

Figure 15: Scenario 01: Efficiency with respect to positions, velocities, and Lagrange multipliers.

3 Summary

On the example of *A Skateboard*, we considered the applicability, efficiency, accuracy, and robustness of different numerical solvers for differential-algebraic equations in combination with several formulations, i.e., regularized formulations or also index reduced formulations, for the model equations.

List of Figures

List of Tables

References

[1] K.E. Brenan, S.L. Campbell, and L.R. Petzold. *Numerical Solution of Initial-Value Problems in Differential Algebraic Equations*, volume 14 of *Classics in Applied Mathematics*. SIAM, Philadelphia, PA, 1996.

[2] E. Eich-Soellner and C. Führer. *Numerical Methods in Multibody Dynamics*. B.G.Teubner, Stuttgart, 1998.

[3] C. Führer. *Differential-algebraische Gleichungssysteme in mechanischen Mehrkörpersystemen - Theorie, numerische Ansätze und Anwendungen*. PhD thesis, Technische Universität München, 1988.

[4] C.W. Gear, B. Leimkuhler, and G.K. Gupta. Automatic integration of Euler-Lagrange equations with constraints. *Journal of Computional and Applied Mathematics*, 12/13:77–90, 1985.

[5] E. Hairer, C. Lubich, and M. Roche. *The Numerical Solution of Differential-Algebraic Systems by Runge-Kutta Methods*. Springer-Verlag, Berlin, Germany, 1989.

[6] E. Hairer and G. Wanner. *Solving Ordinary Differential Equations II - Stiff and Differential-Algebraic Problems*. Springer-Verlag, Berlin, Germany, 2nd edition, 1996.

[7] A. Steinbrecher. *Numerical Solution of Quasi-Linear Differential-Algebraic Equations and Industrial Simulation of Multibody Systems*. PhD thesis, Institute of Mathematics, Technische Universität Berlin, 2006.

[8] A. Steinbrecher. GEOMS: A new software package for the numerical simulation of multibody systems. In *10th International Conference on Computer Modeling and Simulation (EUROSIM/UKSIM 2008)*, pages 643–648. IEEE, 2008.